Ternary Blends of High-Density Polyethylene–Polystyrene–Poly(ethylene/butylene-*b*-styrene) Copolymers: Properties and Orientation Behavior in Plane–Strain Compression

Z. BARTCZAK, A. GALESKI, M. PLUTA

Centre of Molecular and Macromolecular Studies, Polish Academy of Sciences, Sienkiewicza 112, 90-363 Łódź, Poland

Received 9 January 1999; accepted 18 April 1999

ABSTRACT: Ternary blends of high-density polyethylene (HDPE) with atactic polystyrene (PS) and styrene–ethylene/butylene–styrene block copolymer (SEBS) were deformed by plane–strain compression in a channel die. The samples were deformed up to the true strain of 1.8 (compression ratio of 6) at 100°C. Thermal and mechanical properties of the deformed blends were studied in addition to the study of the deformation process. The basic mechanism of plastic deformation is crystallographic slip, the same as that active in deformation of plain HDPE and binary blends of HDPE and PS. This slip is supplemented by the plastic deformation of an amorphous component. In blends of high SEBS content, the role of deformation of an amorphous component by shear and flow increases markedly due to reduced overall crystallinity of these blends. In such blends an amorphous component includes a semicontinuous embedding of crystallites, and therefore, the deformation process is dominated by deformation mechanisms active in a more compliant amorphous phase. Consequently, with increasing the content of SEBS in the blend, the texture of the oriented blends changes from a single-component (100)[001] texture to a texture with a strong fiber component in addition to a (100)[001] component. In blends with high content of SEBS, the crystalline lamellae of polyethylene do not undergo fragmentation up to the compression ratio of 6, while in blends with low and moderate content of SEBS, such lamellar fragmentation was detected. © 2000 John Wiley & Sons, Inc. J Appl Polym Sci 76: 1746–1761, 2000

Key words: blends; plastic deformation; orientation; deformation mechanism; polyethylene; polystyrene; compatibilization

INTRODUCTION

The successful application of polymer blends as engineering materials depends largely on their ability to undergo extensive plastic deformation upon action of high loads. Therefore, the plastic deformation behavior of polymer blends under high or excessive forces is very important. However, the presence of interfaces in blends of immiscible polymers considerably reduces the ability to accept large strain plastic deformation due to usually poor adhesion between blend components. Such poor adhesion is common for many pairs of polymers, and is the source of cavitation of the blend by debonding at interfaces. The cavitation generally contributes to plastic deformation, though a single large cavity may often cause premature cracking of the sample. Consequently, many blends fracture at relatively low strain compared with plain polymers. To improve interphase adhesion and, additionally, the dispersion of blend components, compatibilization tech-

Correspondence to: Z. Bartczak.

Contract grant sponsor: State Committee for Scientific Research (Poland); contract number: 7S20401306.

Journal of Applied Polymer Science, Vol. 76, 1746–1761 (2000)

niques have been developed (see, e.g., refs. 1 and 2). Compatibilization of blend components is commonly achieved by addition of a small quantity of a carefully selected third component to the mixture. That component is usually a graft or block copolymer, the blocks of which show some affinity toward both basic components of the blend.

This article continues our series of studies of plastic deformation of polymer blends. In the previous article,[3] we studied the plastic deformation behavior of blends of high-density polyethylene (HDPE) with atactic polystyrene (PS). The blend of HDPE and PS is a typical immiscible binary blend, with extremely low interphase adhesion, which results in relatively poor dispersion (size of inclusions of PS dispersed in the HDPE matrix is in the range of microns). Although those blends easily exhibit very poor mechanical properties and fracture when tested in a tensile deformation mode, high-strain plastic deformation by plane–strain compression in a channel die is possible. That deformation mode produces strain equivalent to that in the tensile experiments, but the compressive stresses generated within the sample reduce cavitation and debonding phenomena responsible for the fracture in tension. It was found[3] that the deformation mechanisms active in the deformation of the HDPE/PS blend by plane–strain compression are generally the same crystallographic mechanisms as those active in plastic deformation of plain HDPE.[4] These are primarily (100)[001], (100)[010], and (010)[001] crystallographic slip systems, which are supported by interlamellar slip operating in the amorphous component of the HDPE matrix. The presence of PS in blends slightly modifies the deformation process and the resulting orientation of the HDPE matrix by modification of the stress distribution within the HDPE matrix around the PS inclusions. That influence is much stronger at low deformation temperatures, when PS is in a glassy state, than at temperatures above the T_g of the PS, where the PS inclusions are much more compliant than the embedding HDPE matrix.

In this article we attempted to study the deformation behavior of the blends of HDPE and PS compatibilized with styrene–(ethylene/butadiene)–styrene block copolymer (SEBS). SEBS copolymers are known as good compatibilizng agents for polyethylene and polystyrene[5–8] because styrene end blocks are miscible with a polystyrene component while the hydrogenated ethylene/butadiene block exhibits some affinity for HDPE. Addition of an SEBS block copolymer to the blend changes the structure and properties of the interphase between components. This results in an improvement of interphase adhesion,[5] and additionally induces much better dispersion of the PS in the HDPE matrix.[8] It was found[8] that with increasing the content of the SEBS in the HDPE/PS/SEBS blend the size of the inclusions decreases from several microns to less than 0.1μm. Simultaneously, a transformation of the morphology of the blend from isolated droplets to clusters and aggregates was observed. The presence of the SEBS compatibilizer in the HDPE/PS blend improves its mechanical properties and ability to undergo extensive plastic deformation.[5]

The aim of this work was to study the mechanical properties of a compatibilized blend and to find out mechanisms of plastic deformation. The related issues were the influences of the multiphase morphology and the interphase between components on the plastic deformation process and mechanisms active in deformation.

EXPERIMENTAL

The materials used in the present study were high-density polyethylene, HDPE (Lupolen 5261Z, BASF, $M_w = 5 \times 10^5$, $M_w/M_n = 13$, Melt Flow Index 1.8 g/10 min. [21.6 kG at 190°C], density 0.952 g/cm^3), atactic polystyrene, PS (Polystyrol 186N, BASF; $M_w = 3.00 \times 10^5$, $M_n = 1.81 \times 10^5$, Melt Flow Index 1.2 g/10min [5.0 kG at 200°C], density 1.05 g/cm^3, $T_{g,\mathrm{DSC}} = 106$°C), and polystyrene–poly(ethylene/butylene)–polystyrene block copolymer, SEBS (Kraton G1650, $M_w = 9.5 \times 10^4$, M_w of the end segment 1.45×10^4, M_w of the middle segment 7.1×10^4, styrene content 30%, density 0.91 g/cm^3) in which butylene was hydrogenated after copolymerization.

Ternary blends of various compositions were blended by extrusion in a single-screw extruder (L/D = 25; Plasti-Corder PL2000, Brabender) at 220°C. The compositions of the prepared blends are listed in Table I, along with their codes used throughout this article. All blends prepared had a common overall composition: 80 wt % of a polyolefine phase [consisting of HDPE and poly(ethylene/butylene) blocks of SEBS] and 20 wt % of PS phase (consisting of plain PS and PS blocks in SEBS component). Due to the relatively high molecular weight of the components, their melt viscosities at the processing temperature were high. This made the extrusion-blending process difficult. Therefore, to improve the dispersion of the

Table I Composition of the Blend Studied

Blend Code	HDPE (wt %)	PS (wt %)	SEBS (wt %)
KR-0	80	20	0
KR-2	78.6	19.4	2
KR-5	76.5	18.5	5
KR-10	73	17	10
KR-20	66	14	20
KR-40	52	8	40
KR-67	33.3	0	66.7

components, the extrusion process was repeated twice for each composition. The obtained pellets of the blends were compression molded at 180°C and 200 atm to form 12 mm-thick plaques. Subsequently, the mold was slowly cooled down to room temperature. The outer skin layers of the molded plaques (up to 1 mm from each side) were machined to obtain the specimens as rectangular plates 50 × 60 mm and 10 mm thick, suitable for compression tests. As revealed by DSC and X-ray measurements, the obtained plates had crystallinity of polyethylene around 65% and no traces of orientation anisotropy. For tensile tests, oar-shaped specimens were cut out from 1 mm-thick sheets, molded under conditions similar to that described above.

The plane–strain compression in a channel die was chosen as the deformation method in this study. All compression experiments in the channel die were done at a temperature of 100°C. This temperature of deformation was selected on the basis of the previous study of compression of the binary HDPE/PS blend,[3] which demonstrated that the deformation process is stable and leads to high permanent orientation of the material if the temperature is set within the zone of the glass transition temperature of the PS component. The temperature of deformation selected for this study is close to the T_g of both plain PS and PS segments of SEBS (106 and 94°C, respectively). A compressive load to the plunger of the channel die was applied using an Instron Testing Machine Model 1114T. The same crosshead speed of 1 mm/min was used in all experiments (the initial deformation rate, ε, was $2.77 \cdot 10^{-4}s^{-1}$). The compression was ended near the compression ratio of 6 (reduction of the sample height from 60 to 10 mm). Afterwards, the compression samples were slowly cooled to room temperature, still under the load. The other details of the deformation procedure are described elsewhere.[3]

The orientation of the polyethylene crystalline phase in deformed samples was studied by means of X-ray pole figure measurements. A WAXS system, consisting of a computer-controlled pole figure device associated with a wide-angle goniometer (DRON) coupled to a sealed-tube X-ray generator operating at 30 kV and 30 mA (Cu K_α radiation, filtered electronically and by a Ni filter), was used in this study for X-ray measurements. Details of the pole figures determination procedure are described in ref. 3. The following diffraction reflections from the orthorombic crystal structure of polyethylene were analyzed for the construction of pole figures: (200), (020), and (002) (diffraction angle, $2\Theta \approx 24$, 36.4, and 74.4°, respectively). The slit system of the diffractometer was always selected to measure the integral intensity of the appropriate diffraction peak. Necessary corrections for background scattering, sample absorption, X-ray defocusing, and other instrumental effects due to the sample tilt were applied to the raw data. The data obtained at identical experimental conditions for randomly oriented standard specimens (the isotropic specimen of HDPE of the same size and thermal history as the samples studied) were used for defocusing correction. The pole figure plots were generated by the program POD, a part of the popLA package (Los Alamos National Laboratory, Los Alamos, NM). For every plot the data were normalized to the random distribution density.

Two-dimensional small-angle X-ray scattering (SAXS) patterns were recorded using a Siemens Hi-Star area detector controlled by a GADDS software coupled to a 18-kW rotating anode X-ray source (Cu K_α radiation; Rigaku RV-300). The collimator system gave a point focus with a beam diameter of 0.5 mm. The distance between sample holder and detector was 1.25 m. The exposure time was usually set to 90 min. The contour plots of the 2D SAXS patterns were generated from experimental pattens using the modified POD program.

The morphology of virgin as well as oriented samples was examined by scanning electron microscopy (SEM) in samples with planes of interest exposed by freeze-fracture or by cutting with a microtome and etching with toluene to remove the near-surface PS phase.

A DuPont TA-2000 differential scanning calorimeter (DSC) was used to study the crystallization and melting behavior of the specimens. The cooling and heating rates were both set to 10°C/min. For calculation of the overall crystallinity of

polyethylene from the DSC data, the heat of fusion of 100% crystalline polyethylene was taken as $H_f = 293$ J/g.[9]

The mechanical tests of the unoriented blend samples were carried out in the tensile mode at room temperature using an Instron tensile testing machine. Oar-shaped tensile specimens (DIN 53504), with a gauge length of 20 mm, a width of 4 mm, and a thickness of 1 mm, were punched out from the unoriented compression-molded sheets. The deformation rate was 10 mm/min in all tensile tests.

The dynamical mechanical measurements (DMTA) of raw (unoriented) and oriented blend samples were carried out by using a DMTA Mk III apparatus (Rheometric Scientific) operating in a dual-cantilever bending mode at 1 Hz and a heating rate of 2°C/min.

RESULTS AND DISCUSSION

Unoriented Blends

Morphology

The SEM observations of freeze-fracture and/or etched surfaces were used to examine the morphology of blend samples in this study. This technique has severe limitations, because it primarily reveals the topology of fracture surface. Therefore, the real phase morphology of the sample is often obscured by surface features produced by fracture process. These effects may be reduced by fracturing notched samples at liquid nitrogen temperature, which results in a fast, brittle fracture with a smooth surface and little artifacts. Additional etching of the exposed surface can help reveal the phase morphology, although improper etching may produce some additional artifacts (overetching). Usually, more reliable results are obtained when phase morphology is inspected with transmission electron microscopy (TEM) instead of SEM. However, for TEM observations, the blend sample must be properly stained and then sectioned with an ultramicrotome. Our attempts of staining and then sectioning of HDPE/PS/SEBS blend samples did not give satisfactory results, especially in the case of deformed samples. Therefore, we limited our studies to SEM observations only.

Figure 1 shows the morphology of the HDPE/PS/SEBS blends as observed on freeze-fractured surfaces. Figure 1(a) shows that PS in the binary uncompatibilized HDPE/PS blend (KR-0) forms spherical or ellipsoidal particles with diameters in the range from 0.5 to 3 μm, incorporated evenly in the HDPE matrix. The smooth surface of these particles indicates that adhesion between blend components is very low. The morphology of the blend changes gradually with an increasing amount of SEBS—the size of PS inclusions decreases and particles become more irregular in shape and difficult to distinguish from the HDPE matrix due to smearing of the interfaces. Eventually, in sample KR-67, the particle morphology is no longer visible on the fracture surface [cf. Fig. 1(d)]. Multiphase morphology, however, becomes visible after surface etching [cf. Fig. 1(e)]—the aggregates of small SEBS particles (usually smaller than 0.5 μm) are dispersed in the matrix. The above observations agree with those reported by Haaga et al.,[8] who studied the morphology of HDPE/PS/SEBS blends of the same composition as studied here by TEM. They found a decrease of the average particle size from a few microns to less than 0.1 μm with the SEBS content in the blend increasing from 0 to 66.7 wt %. They also noticed a transition of inclusion morphology from separate large particles (in blends with 0–5% of SEBS added) through clusters (5–15% of SEBS) to aggregates of very small inclusions (above 15% of SEBS) with increasing the concentration of SEBS. The morphology of the blends investigated in this study is coarser than reported in ref. 8. This is probably due to a higher molecular mass of HDPE and PS in the blends studied here and less severe mixing of components employed in this study compared with those reported by Haaga et al.[8]

Thermal Behavior

Table II illustrates thermal behavior (nonisothermal crystallization and subsequent melting, as probed by DSC) of the neat HDPE and various HDPE/PS/SEBS blends, all samples unoriented. It is seen that polyethylene in the blend samples crystallizes somewhat faster than in a neat HDPE resin processed at the same conditions as the blends, including an extrusion step. On the other hand, there is almost no difference between crystallization behavior observed for samples of various blend compositions. For any blend sample the temperature of onset of crystallization is approximately 4.5°C higher than that of plain HDPE, while the temperature of the crystallization peak rises in blends as much as 6.5°C above that observed for plain HDPE. The above result

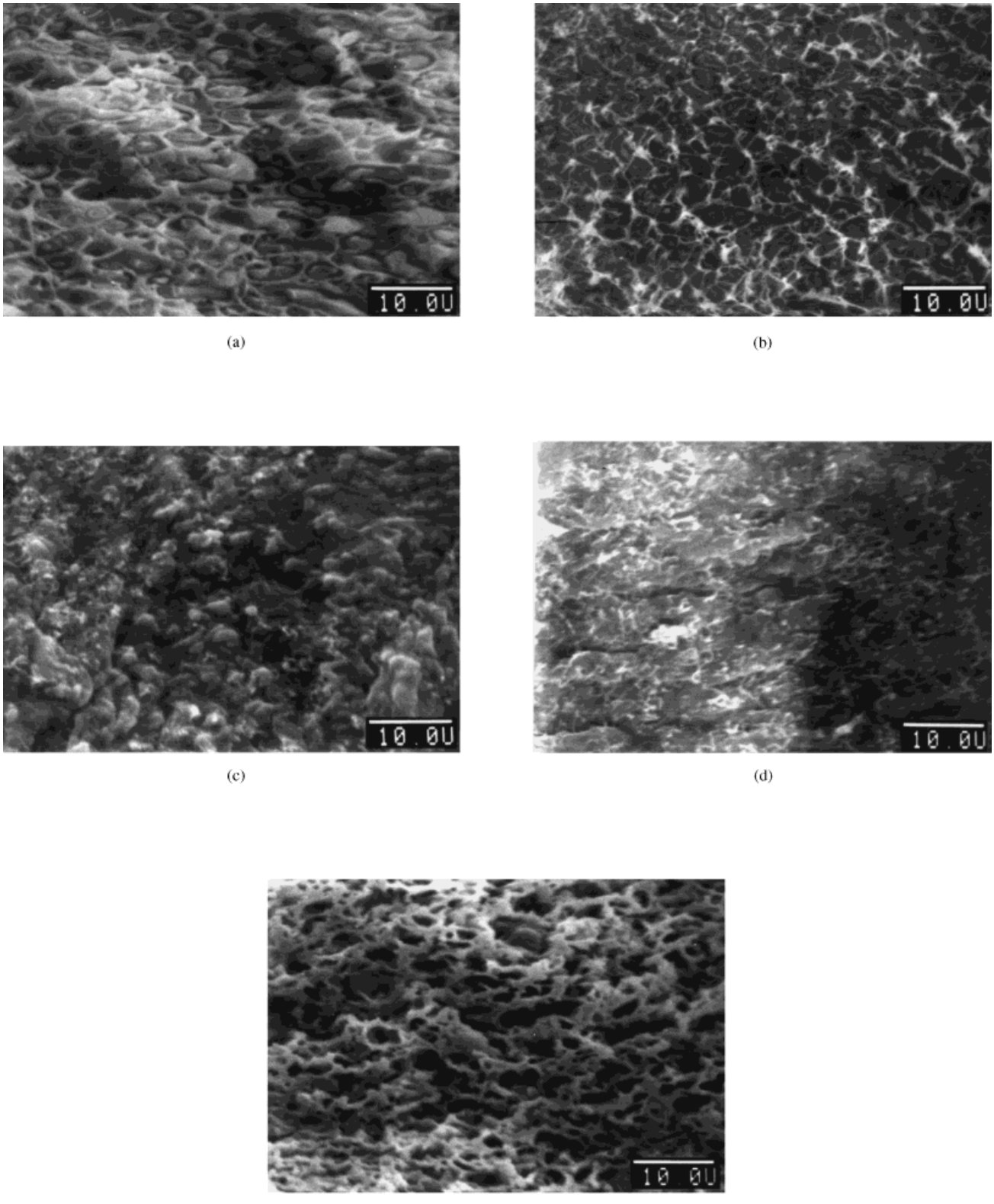

Figure 1 Scanning electron micrographs of the surfaces of freeze-fractured samples of unoriented HDPE/PS/SEBS blends: (a) KR-0, (b) KR-10, (c) KR-40, (d) KR-67, and (e) KR-67 etched with toluene. Scale bar 10 μm.

Table II Crystallization and Melting Data Obtained by DSC in Cooling from the Melt at the Rate of 10°/min and Subsequent Heating at the 10°/min Rate

	Crystallization			Melting		
Blend Code	T_c (onset) (°C)	T_c (peak) (°C)	X_c (HDPE) (%)	T_m (onset) (°C)	T_m (peak) (°C)	X_c (HDPE) (%)
HDPE	122.0	116.9	69.3	124.4	136.8	66.3
KR-0	126.5	123.2	64.0	127.0	134.5	65.5
KR-2	126.6	123.4	65.0	127.1	134.4	67.5
KR-5	126.6	123.5	64.2	126.7	134.1	65.9
KR-10	126.8	123.2	63.1	126.8	134.4	65.0
KR-20	127.2	123.6	61.9	127.0	134.8	65.0
KR-40	126.7	123.3	59.0	127.3	134.8	63.1
KR-67	126.5	123.7	59.4	127.1	134.9	61.2

suggests strong influence of the other component on the crystallization of HDPE in blends, most probably on the primary nucleation of spherulites. The studies of crystallization in similar blends of isotactic polypropylene with PS demonstrates that the presence of PS in a blend causes a substantial increase of the density of primary nucleation, while it does not influence the growth rate of spherulites.[10] Such behavior is a result of a migration of heterogeneities (catalyst remnants, additives, impurities, etc.) constituting potential nucleation sites from PS toward an iPP component during blending of the components. The driving force for that migration is the difference of the interfacial free energy of those heterogeneities against the iPP and PS components, respectively. Similar migration phenomena are probably responsible for the increase of crystallization temperature of the HDPE component in blends reported in this study.

The nonisothermally crystallized blend samples upon heating show a higher onset temperature of melting, yet the temperature of the melting peak is depressed compared with the plain HDPE. The higher onset temperature in the blends reflects their crystallization at a higher temperature. On the other hand, a depression of the melting peak temperature in the blends compared to the plain HDPE suggests that the crystals grown in the blend samples are less perfect than those formed in the plain HDPE. This suggestion can be confirmed by the crystallinity data. Crystallinity, as calculated with respect to the HDPE fraction in the blends, decreases with increasing SEBS content in the blend. This decrease can be observed in the crystallinity degree calculated either from crystallization or melting data. Another reason for the crystallinity decrease in the blends compared with neat HDPE, especially those containing 40 wt % or more of the SEBS copolymer, can be a partial miscibility of HDPE with poly(ethylene/butylene) segments of SEBS within interfacial layers. In these regions conditions for crystallization are much more difficult than in the bulk HDPE due to dilution with poly(ethylene/butylene) segments. DSC and X-ray diffraction studies demonstrate that these segments are not able to crystallize in plain SEBS copolymer or in the blend with HDPE and PS. Such inability for crystallization results from an irregular structure of the poly(ethylene/butylene) segments.[6]

Mechanical Poperties

The samples of the unoriented HDPE/PS/SEBS blends deformed in tension demonstrate vaied deformation and fracture behavior dependent on their composition. Figure 2 presents stress–strain curves of the studied blends tested in tension. The uncompatibilized HDPE/PS blend and the blends with low content of block copolymer (up to 5 wt %) show brittle or semibrittle behavior and fracture before reaching the yield point. With increasing content of the compatibilizer (KR-10, KR-20, 10 and 20 wt % of SEBS, respectively) the samples become ductile, and break shortly after yield at elongation near 20%. When the amount of SEBS increases further (KR-40, KR-67, 40 and 67 wt % of SEBS, respectively) the samples can be elongated easily to an extension of several hundred percent. Table III summarizes tensile properties of raw unoriented HDPE/PS/SEBS blends. It is seen that, with increasing content of a block co-

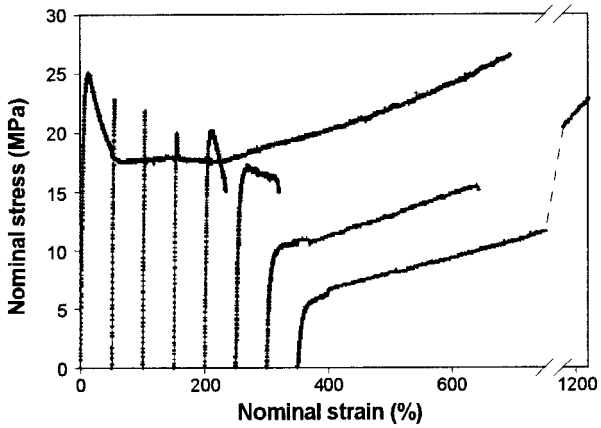

Figure 2 Tensile nominal stress–nominal strain curves of the HDPE and HDPE/PS/SEBS blends. The curves from left to right: HDPE, KR-0, KR-2, KR-5, KR-10, KR-20, KR-40, and KR-67. The curves were shifted along the strain axis for clarity of presentation.

polymer in the blend, both the Young modulus, E, and the yield stress, σ_y (if yield is observed) gradually decrease with increasing the content of the SEBS in the blend. The ultimate strength, σ_b for samples containing up to 20 wt % of the block copolymer decreases similarly to the yield stress and starts to increase again for samples with higher copolymer concentration due to strain hardening observed in these samples at high strains (see curves of KR-40, KR-67 in Fig. 2).

The mechanical properties of blends reported above demonstrate the efficiency of the SEBS block copolymer as a compatibilizing agent for the HDPE-PS system, especially when its concentration in the blend is between 10–20 wt %. Such a conclusion agrees with results of other investigations of the PE/PS/SEBS system.[6,8] The compatibilization mechanism is related to the improved interfacial adhesion between PS inclusions and the HDPE matrix as well as finer dispersion of PS particles in the presence of a block copolymer in the blend. The improved interfacial adhesion results from compatibility of appropriate blocks of the SEBS copolymer with either PS and HDPE. The miscibility of PS end blocks with the PS blend component is obvious. The compatibility of poly(ethylene/butylene) block with HDPE is proven by the shift of temperature of γ and β relaxations observed in blends by dynamical mechanical analysis (DMTA). The results of DMTA studies of unoriented blends are presented in Figue 3. Table IV summarizes the temperatures of the relaxations determined from DMTA curves using a peak separation procedure for determination of the positions of the relaxation maxima. The relaxations depicted in this table as γ and β are observed in HDPE and in poly(ethylene/butylene) segments of the SEBS copolymer at nearly the same temperatures, because both are polyolefins of quite similar structure. However, the β relaxation peak of HDPE is extremely low compared with poly(ethylene/butylene) segments due to its high crystallinity.[11] The data presented in Table IV show that going from plain HDPE through blends with increasing content of the copolymer to plain SEBS, the temperature of the γ relaxation tends to increase gradually, while the temperature of the β relaxation tends to decrease. Such behavior supports the idea of partial miscibility of EB blocks with the HDPE matrix in the blend. One must note that the shift of position of the β relaxation with composition is very small—in fact, not far from experimental error. However, it was confirmed in several repeated DMTA scans. To refine the position of the maxima, a curve-fitting procedure was used. The deviations of position of the β maximum, found in subsequent experiments, did not deviate more than 0.3°C from those reported in Table IV.

Table III Tensile Properties of Unoriented HDPE/PS/SEBS Blends

Blend Code	SEBS Content (wt %)	E (MPa)	σ_y (MPa)	σ_b (MPa)	ε_b (%)
KR-0	0	628	—	22.1	6
KR-2	2	551	—	19.3	6
KR-5	5	528	21.2	20.1	12
KR-10	10	416	19.2	18.7	18
KR-20	20	343	16.5	16.2	23
KR-40	40	146	11.5	29.4	600
KR-67	66.7	46	6.0	38.0	>1000

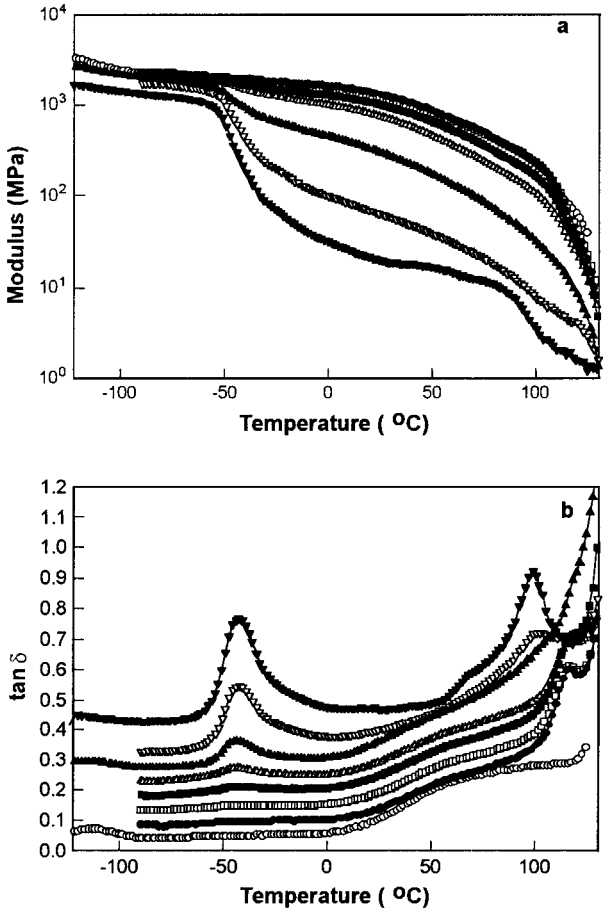

Figure 3 Dependence of the dynamic storage modulus, E' (a) and dynamic loss, tan δ (b) on temperature determined for unoriented samples by DMTA in bending mode at 1 Hz: (○) HDPE, (●) KR-0, (□) KR-5, (■) KR-10, (△) KR-20, (▲) KR-40, (▽) KR-67, (▼) SEBS. The curves of tan δ are shiftet by 0.05 along the vertical axis (0.1 for SEBS) for clarity.

Deformation of a Blend by Plane–Strain Compression

The samples of blends of various compositions were deformed plastically by compression in a channel die. Such a method of deformation is the realization of plane–strain deformation: a sample changes its size in two directions during the deformation (contracting in the loading direction, LD, and expanding in the flow direction, FD), while its dimension along the transverse direction, CD, remains unchanged due to constraints imposed on deformation by the side walls of a channel die.

The deformation process was done at 100°C. This temperature of deformation was chosen because it coincides with the transition zone between the glassy and rubbery state of the PS segments (glass transition temperatures of the PS segments of the SEBS block copolymer and of the PS homopolymer are 94 and 106°C, respectively, as revealed by DSC). Previous investigations of HDPE/PS binary blends[3] demonstrated that when the deformation temperature was selected within this transition zone, the PS particles were neither too stiff nor too soft to markedly influence the deformation of the HDPE matrix, as opposed to deformations well below or well above the glass transition temperature of the PS. Consequently, the deformation process at a temperature close to the T_g of the PS component was stable, and led to a high permanent orientation of the samples.

Figure 4 shows an example of true stress–true strain curves of the blend samples compressed to the permanent true strain 1.8 (equivalent to the compression ratio of 6). The similar shape of all curves suggests similar deformation behavior of every blend composition studied. Decreasing yield and flow stresses with an increase of the SEBS content reflects an increasing amount of the relative soft amorphous phase originating from the ethylene/butylene segments of SEBS.

The morphology of the deformed samples is presented in Figure 5. The SEM micrographs show sections through the FD–LD plane in deformed specimens, exposed with a microtome and then etched with toluene to remove the near-surface PS and SEBS (the near-surface SEBS is etched only partially). Due to etching, one can observe on micrographs the vacancies left by dissolved PS inclusions. In all cross-sections along the FD–LD plane the elongated traces of deformed inclusions are visible. In sections cut parallel to the LD–TD plane (not shown here), traces of inclusions flattened in the direction of loading were observed. The SEM observations indicate that PS inclusions underwent plastic deformation to the strain close to the overall strain—the inclusions are elongated in the flow direction and contracted in the loading direction, while their size along the constrain direction remains nearly unchanged. The SEM micrographs also show the presence of curved fibrils around the inclusions. This demonstrates that in the vicinity of inclusions there was a considerable distortion of the otherwise uniform strain field, and therefore, a distortion of orientation of the HDPE matrix.

Figure 6 presents the pole figures of basic crystallographic planes of (200), (020), and (002) of

Table IV Temperatures of Relaxations as Determined from DMTA Data (1 Hz) by Peak Fitting Procedure

	Raw (Unoriented) Samples					Oriented Samples		
Blend Code	γ PE + SEBS	β PE + SEBS	α PE	α SEBS	α PS	γ PE + SEBS	β PE + SEBS	α PS
HDPE	−112.6	−44.0	63.5	—	—	−114.6	−42.0	—
KR-0		−43.4	60.5	—	116.8	−113.3	−42.1	112.4
KR-5		−43.9	60.8	—	116.4	−116.4	−42.5	111.9
KR-10		−44.5	61.1	—	116.8	−116.0	−42.8	110.7
KR-20		−43.6	57.2	—	117.4	−117.2	−42.3	111.3
KR-40	−118.2	−43.7	57.1	99.6	117.0	−117.5	−42.4	112.9
KR-67		−42.7	61.0	99.8	—	−117.7	−42.8	—
SEBS	−120.0	−42.9		95.0	—	—		
PS	—	—	—	—	116.2	—		

orthorhombic modification of polyethylene crystals, determined for deformed blend samples. The normal to the (002) plane coincides with the **c** crystallographic axis, which is equivalent to the direction of chains in the polyethylene crystals. Therefore, the (002) pole figure is related directly to the distribution of molecular orientation within the crystalline phase. The pole figures presented in Figure 6 demonstrate that the texture of the deformed blend samples does not substantially change with the blend composition. For every composition, the **c** axis is oriented along the flow direction, while normals to (200) and (020) planes concentrate in the LD–TD plane. Normals to (200) planes form a maximum around LD, while normals to (020) planes concentrate in the CD direction. These maxima are developed best (i.e., are the highest and narrowest) in KR-0 and KR-5 samples, i.e., samples with 0 and 5% of SEBS added to the blend, respectively. The above described features are characteristic for a single-component texture similar to that observed in the plain HDPE deformed at the same conditions.[4,12] One can note, however, that with increasing the content of the SEBS in the blend, the texture of the crystalline phase is less developed [maxima observed in (200) and (020) pole figures are lower]. Moreover, it tends to transform from a single component to a fiber-like texture at a higher concentration of the copolymer in the blend. This evolution is clearly seen in pole figures of the (200) plane—the texture in the HDPE/PS binary blend (KR-0) is relatively sharp, close to that observed in the deformed plain HDPE,[4] while in samples KR-40 and KR-67, the pole figures of the (200) plane suggest rather a fiber-like texture with only weak concentration of normals in the direction close to LD. This demonstrates that constraints imposed on deformation of PE crystals by the side walls of a channel die are much less effective in samples with a high concentration of the block copolymer (40 wt % or more). In such samples the crystalline component of HDPE is a minor blend phase (overall crystallinity degree of the blend is only 20–30%), and HDPE crystallites can be considered as single entities or small crystal–amorphous–crystal stacks embedded in a

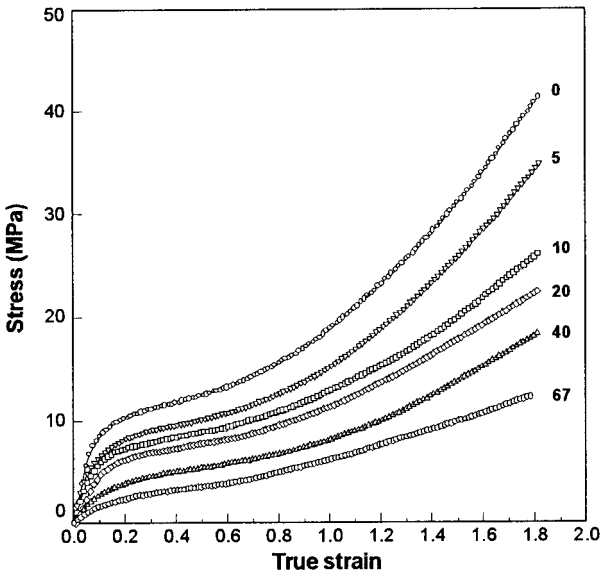

Figure 4 Typical stress–true strain curves ($e = \ln(h_o/h)$) of HDPE/PS/SEBS blend samples deformed by plane–strain compression in a channel die. The numbers on the curves indicate blends: (0) KR-0, (5) KR-5, (10) KR-10, (20) KR-20, (40) KR-40, (67) KR-67.

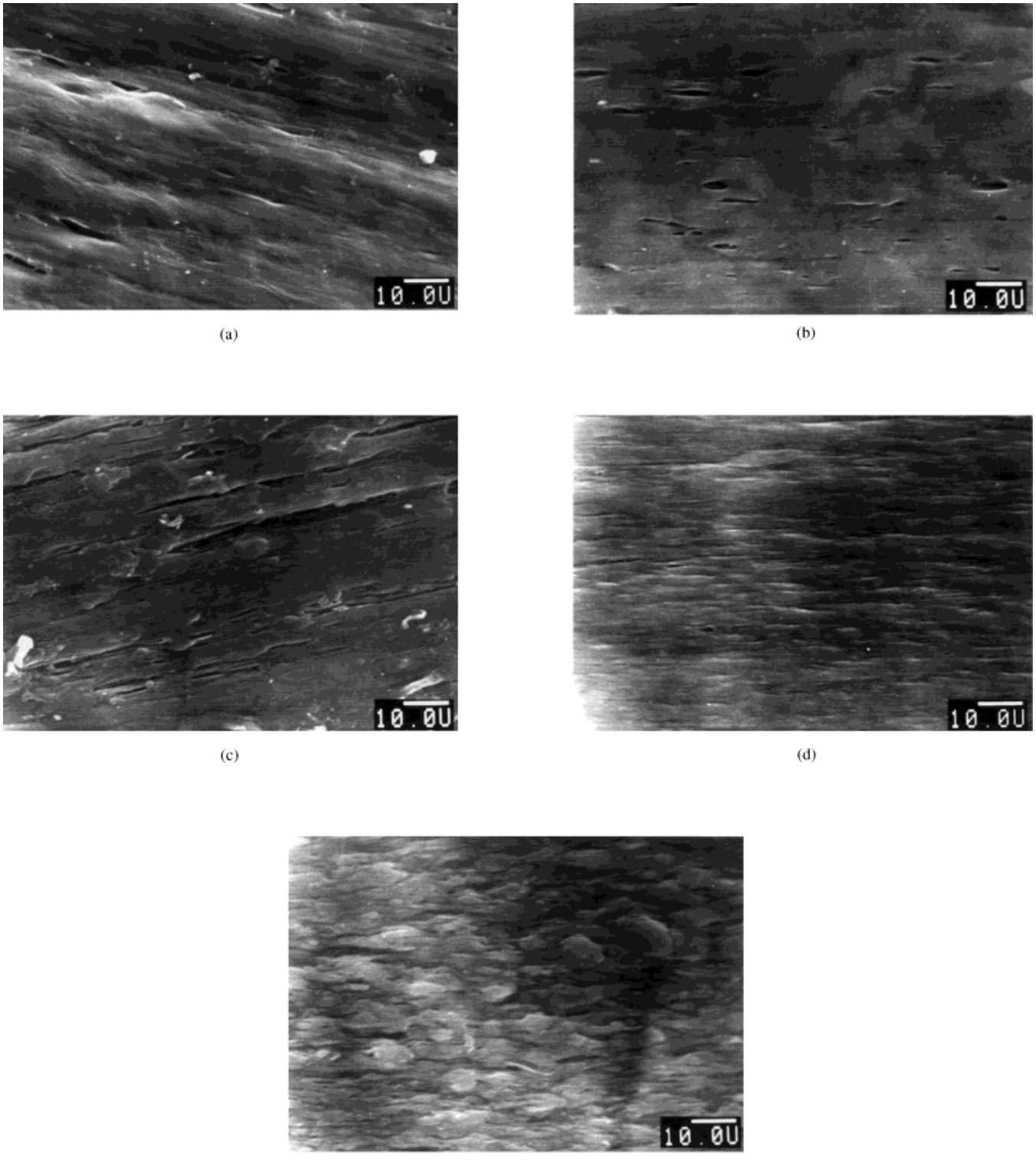

Figure 5 Scanning electron micrographs of the surfaces revealed by cutting the FD–LD plane parallel and etched with toluene of samples of HDPE/PS/SEBS blends oriented by plane–strain compression in a channel die: (a) KR-5, (b) KR-10, (c) KR-20, (d) KR-40 and (e) KR-67. Scale bar 10 μm.

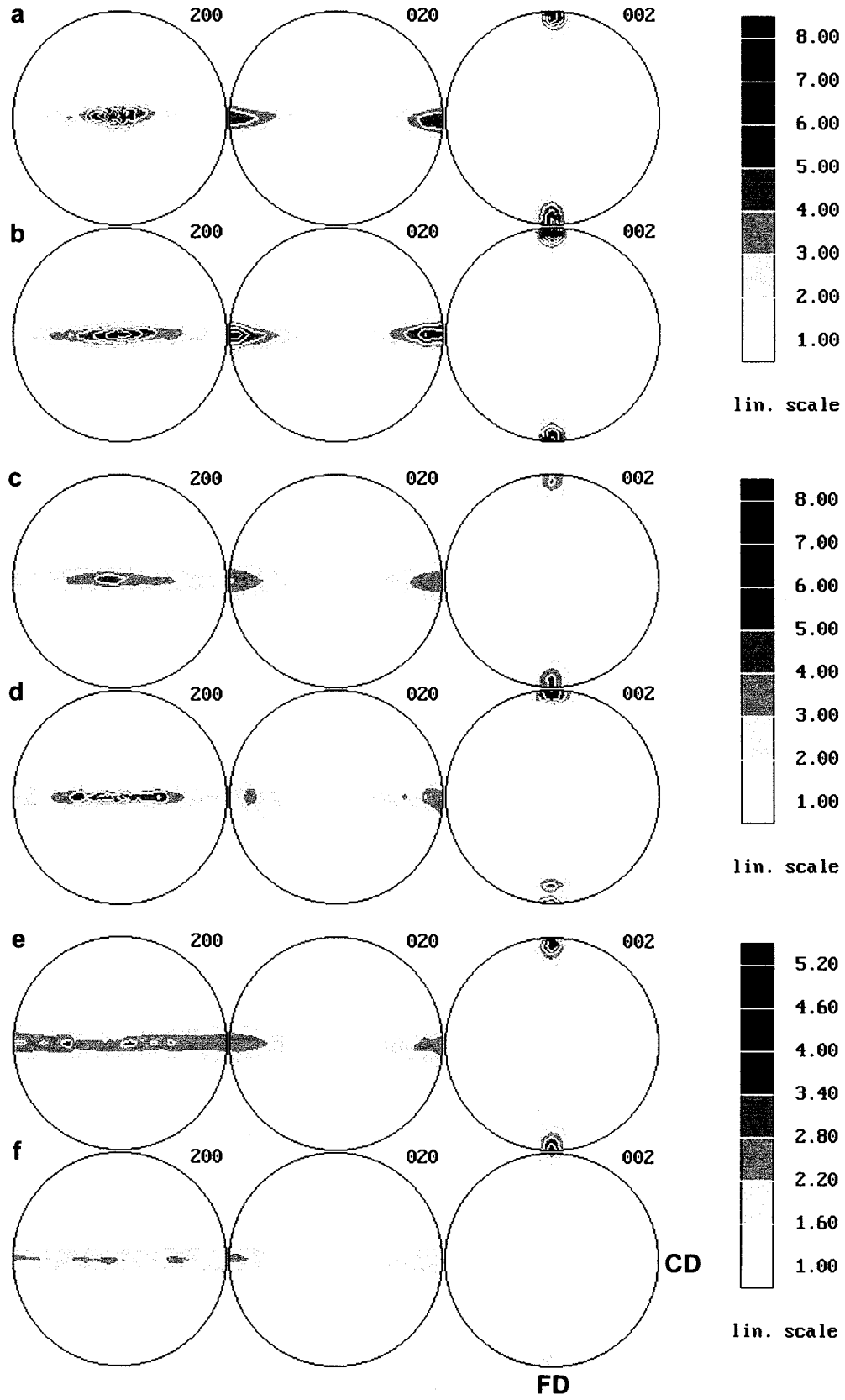
a
200
020
002
b
200
020
002
8.00
7.00
6.00
5.00
4.00
3.00
2.00
1.00
lin. scale
c
200
020
002
d
200
020
002
8.00
7.00
6.00
5.00
4.00
3.00
2.00
1.00
lin. scale
e
200
020
002
f
200
020
002
CD
FD
5.20
4.60
4.00
3.40
2.80
2.20
1.60
1.00
lin. scale

Figure 6

semicontinuous rubbery phase consisting of amorphous PE, SEBS, and PS (PS component is in the transition region between the glassy and rubbery states at the temperature of deformation; PE is rubbery at that temperature). As a consequence of such a phase structure of the blend, the plastic shear and flow of the amorphous component, causing reorientation of the embedded crystallites in the flow field, becomes as important an orientation mechanism of the crystals as the deformation of these crystals by crystallographic slips. Consequently, the side constrains imposed on the crystalline phase by the channel die walls are less effective than in the deformation of highly crystalline material in which orientation of the crystalline phase results primarily from operation of crystallographic mechanisms, much more direction sensitive than the shear and flow of an amorphous rubbery phase. Moreover, when a sample is loaded, an additional hydrostatic stress component is generated within that liquid-like embedding matrix and transmitted to surfaces of crystalline–amorphous blocks. This stress component alters the conditions for plastic shear of the lamellar crystallites. The reorientation of crystallites generated by shear and flow of their amorphous embedding and also plastic deformation of these crystallites by crystallographic mechanisms, proceeding at conditions modified by additional stress components, leads to modification of the final texture of the blend sample from a single-component texture, characteristic for plain HDPE and binary HDPE/PS blends, toward a fiber-like texture, observed in blends of high concentration of SEBS. Some confirmation of such explanation can be additionally found in the SAXS results discussed below.

Figure 7 presents two-dimensional SAXS patterns obtained for oriented blends, taken for two orientations of a specimen with respect to the incident X-ray beam. One of these is an orientation with the FD–CD plane perpendicular to the incident beam (LD—illumination), the other is with the FD–LD plane perpendicular to the beam (CD— illumination). To give more details, the patterns of Figure 7 are supplemented with the intensity profiles determined from these SAXS patterns along the FD, CD, and LD directions, respectively, as presented in Figure 8. The patterns obtained for the KR-0, KR-5, and KR-10 samples show similar features, and are akin to the SAXS patterns observed for plain HDPE deformed in a channel die to a comparable strain:[4,12] a sharp two-point pattern observed when the sample was illuminated from the LD direction, and the pattern consisting of two lines instead of points when the sample was illuminated from the CD direction. The lamellar structure deduced from the very similar scattering patterns of oriented plain polyethylene and confirmed by direct TEM observations[12] is characterized by lamellae oriented quite perpendicularly to the flow direction (more precisely, the projection of their normals on the FD–CD plane is parallel to the FD), while the projections of normals in the FD–LD form some distribution around FD. Moreover, the lamellae are relatively long in the TD, while they are much shorter in the LD, which reflects their fragmentation during the deformation process.[4]

In the blend containing 20 wt % and more of SEBS, the features of the SAXS pattern characteristic of the above-described orientation gradually diminishes while some new maxima start to develop in the LD and CD directions in the respective patterns. These new maxima are best developed in the KR-67 sample, in which the intensity of the scattering at its maximum is somewhat higher than the intensity at maxima produced by the samples of lower SEBS concentration (see Fig. 8). Detailed inspection of the reported maximum in the KR-67 sample revealed that every maximum, in fact, consists of two strongly overlapping maxima each distanced a few degree apart from the LD or from the CD in the patterns obtained for CD and LD illuminations, respectively. This equatorial scattering does not originate from the presence of the voids in the samples, because the scattering characteristic for voids is usually diffused, and does not produce any maximum, in contrast to that observed in the discussed samples. Moreover, in the deformation by compression, such voids are un-

Figure 6 Pole figures of (200), (020), and (002) planes of orthorombic polyethylene crystals (left, center, and right column, respectively) determined for the KR-0 (a), KR-5 (b), KR-10 (c), KR-20 (d), KR-40 (e), and KR-67 (f) blend samples deformed by plane strain compression to the true strain around 1.8 (compression ratio around 6). All pole figures were plotted in stereographical projection, with the flow direction, FD, being vertical, and constrained (transverse) direction, CD, horizontal.

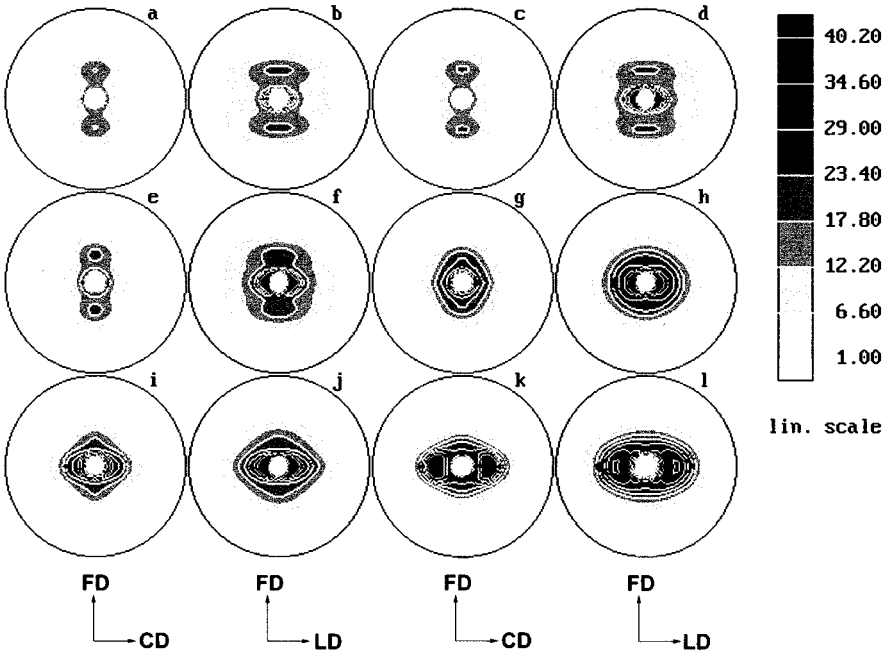

Figure 7 Two-dimensional SAXS patterns of the KR-0 (a,b), KR-5 (c,d), KR-10 (e,f), KR-20 (g,h), KR-40 (i,j), and KR-67 (k,l) samples. Patterns a, c, e, g, i, and k were obtained for samples oriented with loading direction (LD) along the incident beam (flow direction, FD, is vertical, and constrained direction, CD, is horizontal in these patterns), while patterns b, d, f, h, j, and l were oriented with CD along the incident beam (FD is vertical and LD is horizontal).

likely to form. In fact, the comparison of the densities of raw (prior to orientation) and oriented specimens excluds the possibility of the presence of any substantial amount of voids or microcavities in the deformed specimens. The discussed scattering in LD and TD directions in these samples most probably results from the orientation of the lamellae induced by the intense shear and/or flow within semicontinuous amorphous phase embedding crystallites, which causes reorientation of entire lamellae or their stacks. Due to reduced effectiveness of the side constrains, discussed above, the patterns observed in the LD and TD illuminations do not substantially differ. The relative high intensity of the scattering suggests that the lamellae were not yet fragmented at this deformation stage, contrary to the blend with a low content of SEBS or plain HDPE, in which the fragmentation resulted from highly advanced crystal deformation by a chain slip mechanism. The above concepts agree with the previously discussed changes in the orientation of crystallites in blends with a high content of SEBS. One must note, however, that the respective pole figures show that the chains are mostly oriented in the flow direction. On the other hand, the lamellae are oriented with their normals only a few degrees from LD and CD in patterns recorded in CD and LD illumination, respectively. This indicates that the chains are extremely tilted within lamellae, which in turn, demonstrates that the crystallographic slip mechanisms had to be active during plastic deformation (only the crystallographic slip along the chain direction could produce such change of the chain tilt in the lamella). In plain HDPE deformed by plane–strain compression, similar orientation features were observed around a compression ratio of 3.1, at which the intense lamellar fragmentation took place, followed by reconstitution of the long period in the direction of flow at higher compressions.[4] The observations discussed here lead to the conclusion that the crystallographic slip processes are suppressed in samples of a blend with a high content of SEBS and replaced partially by the reorientation of the entire crystals or even their stacks, produced by the plastic deformation of the amorphous embedding, to which the crystals are connected. Such a deformation mode is easier to activate than crystallographic mechanisms in the

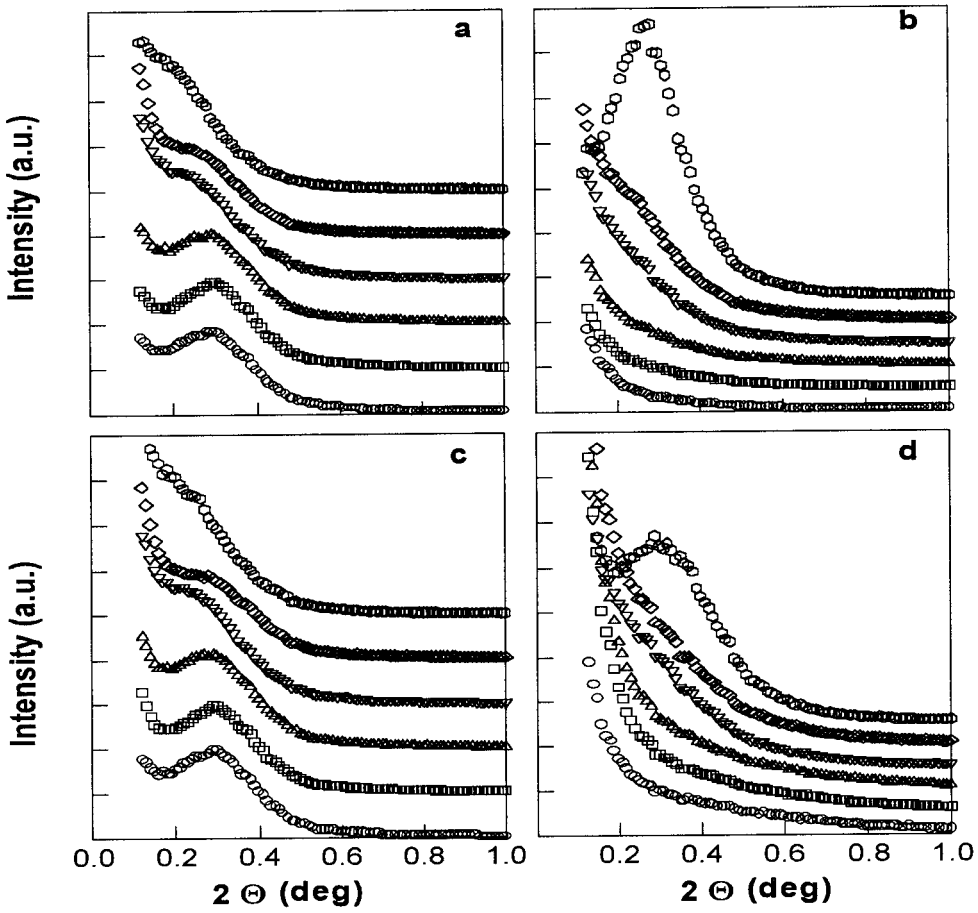

Figure 8 The SAXS intensity profiles (cross-sections of patterns presented in Fig. 7): (a) section along FD when sample is illuminated along the LD, (b) CD section of the same illumination, (c) FD section when sample is illuminated along the CD, (d) LD section of the same illumination. The symbols used are: (○) KR-0, (□) KR-5, (△) KR-10, (▽) KR-20, (◇) KR-40, (hexagon) KR-67.

samples of low crystallinity, especially if the entire amorphous phase is in the rubbery state, as in the case of the KR-67 blend (there is no plain PS in this blend, and glass transition temperatures of E/B and PS blocks are both lower than the temperature of deformation (94 against 100°C).

Examination of 2-D SAXS patterns together with pole figures obtained for the studied blends suggest that, in samples of low content of SEBS the plastic deformation of crystallites through crystallographic slips was the major deformation mechanism, similarly to the deformation of plain HDPE. At a certain strain an advanced crystallographic slip resulted in fragmentation of lamellae due to some instabilities of that slip. In the following stage of the deformation process fragmented crystallites could rotate and deformed further, which resulted in reconstruction of the long period, now in the direction of flow, FD. In contrast, in blends of high SEBS content, relative easy rotation of lamellar crystals or entire stacks were possible due to plastic flow of their amorphous embedding matrix. The plastic deformation of these crystallites by crystallographic mechanisms was rather a secondary source of their orientation. Consequently, the slip processes were advanced less in these blends, and no fragmentation of lamellae and reconstruction of the long period in LD took place during the deformation process of the blends of the high content of SEBS.

Table V presents the melting behavior of specimens of a raw unoriented blend, which were annealed at the temperature of 100°C (i.e., the same as the temperature of deformation), and specimens deformed by plane–strain compression at

Table V DSC Melting Data of Raw (Prior to Orientation) Annealed at 100°C and Samples Oriented at 100°C

	Annealed Samples		Oriented Samples	
Blend Code	T_m (peak) (°C)	X_c (HDPE) (%)	T_m (peak) (°C)	X_c (HDPE) (%)
KR-0	133.4	64.8	137.1	70.1
KR-5	133.8	66.1	137.6	66.4
KR-10	133.9	65.7	138.0	65.7
KR-20	134.3	66.7	136.1	67.1
KR-40	132.9	62.8	136.4	67.0
KR-67	132.0	65.4	133.7	68.1

T_d = 100°C to the compression ratio of 6 (true strain of 1.8). Because of the annealing of unoriented specimens, both sets of samples had the same thermal history. Therefore, the differences of thermal properties of oriented and raw samples primarily result from the deformation process. It is seen that for any blend composition both the melting temperature and crystallinity degree of the deformed samples are higher than that of the unoriented samples of the same composition. Higher melting temperature of the oriented samples reflects destruction of some fraction of the smallest crystallites during the deformation process, while thicker crystallites survived the deformation. Such observations were made also for the deformation of plain HDPE[4] as well as binary HDPE/PS blends.[3] In these studies an increase of temperature of the melting peak was accompanied by a slight decrease of the crystallinity degree of HDPE, which additionally supported the hypothesis of the destruction of some of lamellar crystals. However, in the study reported here, the behavior of the blends is different—crystallinity of HDPE in the deformed blend samples is higher than in the unoriented samples of the same composition.

Figure 9 presents the dynamic mechanical spectra of oriented samples of the blends. It can be seen that these oriented blend samples exhibit several relaxation transitions, all characteristic for blend components, similarly to unoriented samples (cf. Fig. 3). The γ, β, and α relaxations of HDPE are seen as well as the α relaxation of PS component. The γ and β relaxations of HDPE coincide with the respective relaxation processes in ethylene/butylene segments of SEBS. Table IV collects the temperatures of relaxation maxima determined for oriented samples from the DMTA data presented in Figure 9. The increase in γ and β relaxation temperatures can be observed compared with undeformed materials. It is rather clear that this increase resulted from better packing of macromolecules both in the amorphous component and in interphase layers that substantially reduced the mobility of these macromolecules. On the contrary, the temperature of the α relaxation of the PS component in the oriented samples decreases when compared with the unoriented samples. The α relaxation process of PS could, however, be affected by the shrinkage phenomenon occurring in the oriented samples at temperatures around and above the temperature of deformation, i.e., 100°C. This shrinkage possi-

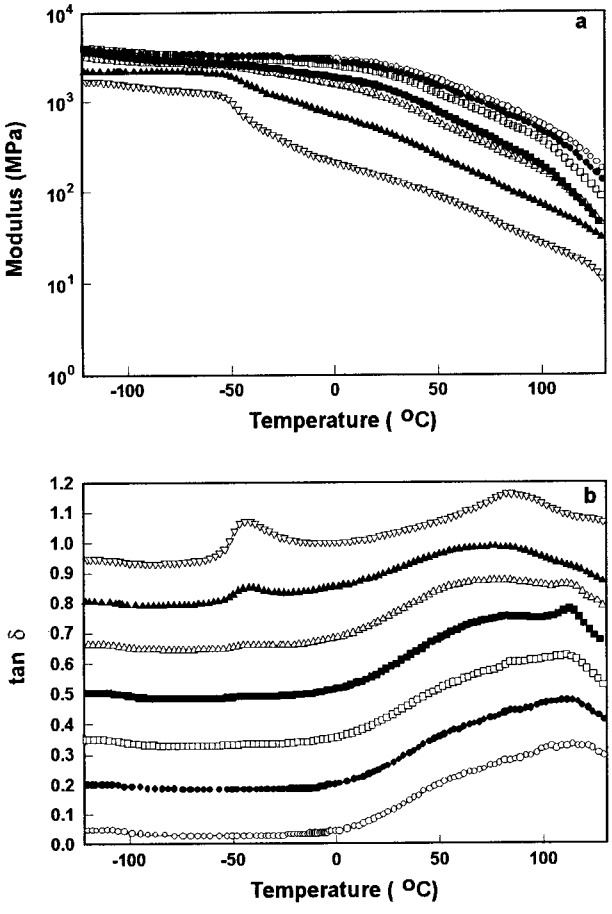

Figure 9 Dependence of the dynamic storage modulus, E' (a) and dynamic loss, tan δ (b) on temperature determined for oriented samples by DMTA in a bending mode at 1 Hz: (○) HDPE, (●) KR-0, (□) KR-5, (■) KR-10, (△) KR-20, (▲) KR-40, (▽) KR- 67. The curves of tan δ are shifted by 0.15 along the vertical axis for clarity of presentation.

bly influenced our estimate of the temperature of the α relaxation process. Probably for the same reason the estimations of the temperatures of the α relaxation of HDPE and the α relaxation of the PS segments in SEBS were inaccurate, and did not show any noticeable correlation.

CONCLUSIONS

The plastic deformation of HDPE/PS blends compatibilized with the SEBS block copolymer, deformed by compression in a channel die, occurs in a cavity-free manner. The compression is plane–strain due to strong constraints imposed by the side walls of the channel. Because of the presence of a compatibilizer in the blends, the interphases between the main blend components do not cavitate and preserve their integrity, although they undergo extensive deformation comparable to the HDPE embedding.

The texture developed by compression to high strains in ternary blends with small and moderate amounts of SEBS is similar to the texture found in plain HDPE and HDPE/PS blends deformed at similar conditions. This is a single-component texture with the chain direction [001] aligned well along the flow direction and the (100) crystallographic plane perpendicular to the loading direction, i.e., the (100)[001] texture. It was found that the basic mechanisms of the plastic deformation of blends are crystallographic slip supplemented by plastic shear and a flow of amorphous component, similar to the deformation of plain polymers and uncompatibilized blends. With increasing content of SEBS in the blend, the texture of the deformed samples evolves toward a fiber-like texture, with [001] still well aligned along the FD. However, the main (100)[001] texture component, although weaker, can still be observed. Such evolution demonstrates an increasing role of the plastic shear and flow of the amorphous component of the blend, at the expense of crystallographic mechanisms in samples of reduced overall crystallinity, as in blends with high SEBS content. For that deformation mode the side constraints imposed by the side walls of the channel are not as effective as in the deformation of highly crystalline material. Consequently, the texture of the blends with increasing concentration of SEBS transforms from a single-component (100)[001] texture to that with a strong fiber component in addition to a (100)[001] texture component. It was also found that the increasing role of deformation of an amorphous phase in the blends of a high content of SEBS inhibits the fragmentation of the lamellar crystals during the deformation process and reconstruction of the long period along the flow direction, while in highly crystalline blends of a low content of SEBS such lamellae fragmentation and restructurization was observed to occur, similar to that found in plane–strain compression of plain HDPE.

This research was supported by the State Committee for Scientific Research (Poland) through project 7S20401306. SAXS measurements performed by M. Pluta at the Max-Planck-Institut für Polymerforschung, Mainz (Germany) were made possible by a DAAD Fellowship and Professor T. Pakula.

REFERENCES

1. Barlow, J. W.; Paul, D. R. Polym Eng Sci 1984, 24, 525.
2. Bonner, J. G.; Hope, P. S. In Polymer Blends and Alloys; Folkes, M. J.; Hope, P. S., Eds.; Chapman & Hall: London, 1993.
3. Bartczak, Z.; Krasnikova, N. P.; Galeski, A. J Appl Polym Sci 1996, 62, 167.
4. Galeski, A.; Bartczak, Z.; Argon, A. S.; Cohen, R. E. Macromolecules 1992, 25, 5705.
5. Lindsey, C. R.; Paul, D. R.; Barlow, J. W. J Appl Polym Sci 1981, 26, 1.
6. Fayt, R.; Jerome, R.; Teyssie, Ph. J Polym Sci Polym Phys Ed 1981, 19, 1269.
7. Welander, M.; Rigdahl, M. Polymer 1989, 30, 207.
8. Haaga, S.; Schneider, H. A.; Friedrich, Ch. Polym Preprints 1993, 34, 799.
9. Wunderlich, B.; Cormier, C. M. J Polym Sci Polym Phys Ed 1967, A-2, 987.
10. Bartczak, Z.; Galeski, A.; Krasnikova, N. P. Polymer 1987, 28, 1627.
11. Boyd, R. H. Polymer 1985, 26, 323.
12. Song, H. H.; Argon, A. S.; Cohen, R. E. Macromolecules 1990, 23, 870.